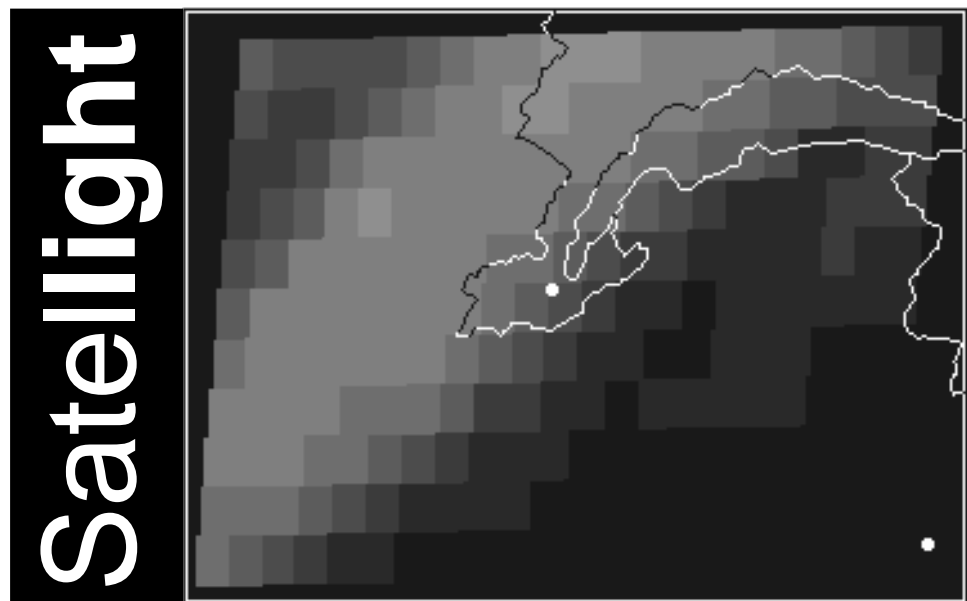


Satellite

Commission of the European Communities

Use of Meteosat data to produce sky luminance maps

Second Satellite meeting
Bergen, June 24-25, 1996



Report prepared by Pierre Ineichen
GAP - Energy / University of Geneva
Switzerland

June 1996

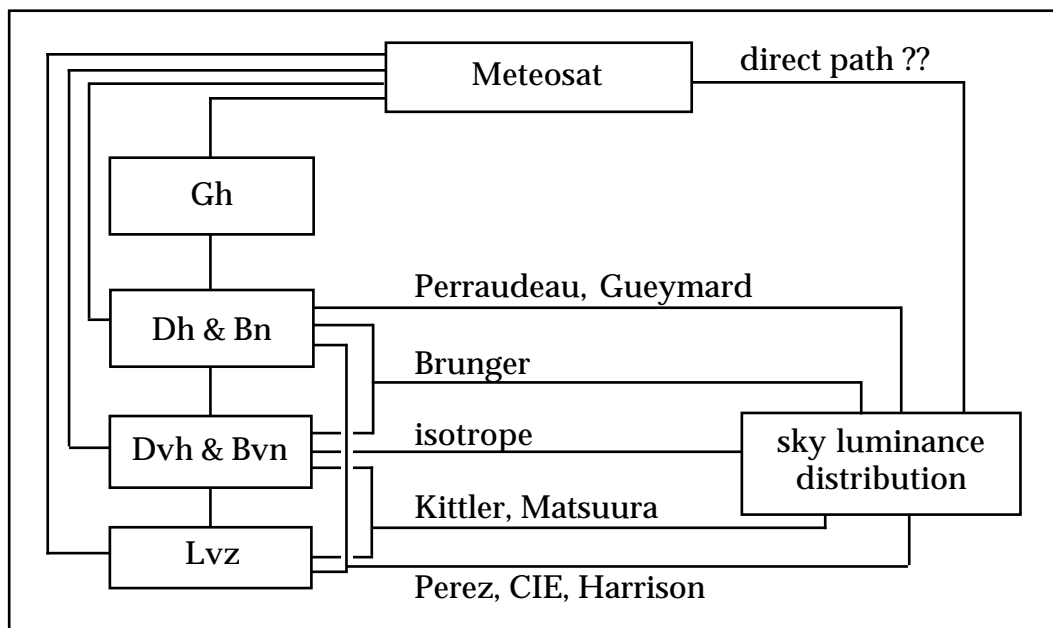
Objectives

The objective of the subtask is to derive a model to evaluate the luminance distribution of the sky vault on the basis of Meteosat data. This information is a key element in the field of building energy saving, it is the basis of indoor daylight calculation. Evaluation programs like Genelux (LASH-ENTPE) need this sky luminance distribution to perform their calculations.

Sky luminance distribution models have been developed in the last years on the basis of horizontal diffuse illuminance. Their precision depends on the input data and these models cannot take into account the statistical cloud distribution in the sky vault. Perez et al. tried to superpose a statistical cloud distribution on their symmetrical model, but this was done on a unique set of data and a particular site. The model was not tested on other data (due to the lack of clean and complete sky luminance distribution database) and therefore cannot be used in any site by now without a question mark on the results.

At the end of the **satellight** project, illuminance and luminance data will be available on line on an Internet server for any location in Europe. Therefore, the only basis of daylight evaluation will be the meteosat images (with a half hourly frequency for the 5x5 km resolution and an hourly frequency for the 2.5x2.5 scale).

There are multiple paths to go from the pixel information to a sky luminance distribution as it was discussed in the Lyon first **satellight** meeting.



We will try to go the straight line from Meteosat pixels to the sky luminance distribution.

Data

Sky luminance distributions have been measured in Geneva in a continuous way since 1991 with a PRC Krochmann sky scanner. The Geneva station is a CIE research class station and the radiation and meteorological parameters are acquired according to the CIE recommendation Guide [CIE, 1994].

The sky scans are done every 15 minute, in 145 different directions. A single scan takes about 35 seconds and the irradiance and illuminance corresponding parameters are measured within the same minute. In 1993, we added an EKO sky scanner. This scanner takes 2.5 minutes for a single scan, and has the possibility to record also the radiance distribution. As we described it in a previous study [Ineichen, 1993], the two instruments are very different and one have to take particular attention to the instruments specifications when developing and testing sky distribution models. We encountered the same kind of situation in the field of radiation model. Indeed, sophisticated models gave better results with high precision input data (for example using beam radiation instead of shading ring corrected diffuse irradiance to evaluate tilted radiation), when very simple models were more reliable with lower precision input data (see for example Perez 1987 and Hay 1978 tilted plane radiation model).

In this study we will use the year 1994 acquired at the Geneva station, including PRC and EKO measurements for the development of a sky luminance distribution model.

There are only two sites in Europe acquiring continuous data of the sky luminance distribution: Geneva since 1991 and Garston (UK) from July 1991 to December 1992. The Garston measurements were done with a PRC Krochmann sky scanner every 15 minute. In a second step we will try to apply the model on the second sky luminance data set. The complementary parameters are integrated and recorded within 2.5 minutes from the scan.

Quality control

The first step in any model development or testing is the calibration and the quality control of the data. After a severe quality control on the Gh/Dh/Bn irradiances and illuminances, one can compare the horizontal diffuse illuminance with the integral of the scan. Due to the non-zero aperture angle and the dynamic sensitivity of the sensor, the measurements done very near from the sun direction ($\zeta < 12$, angular distance between the measurement

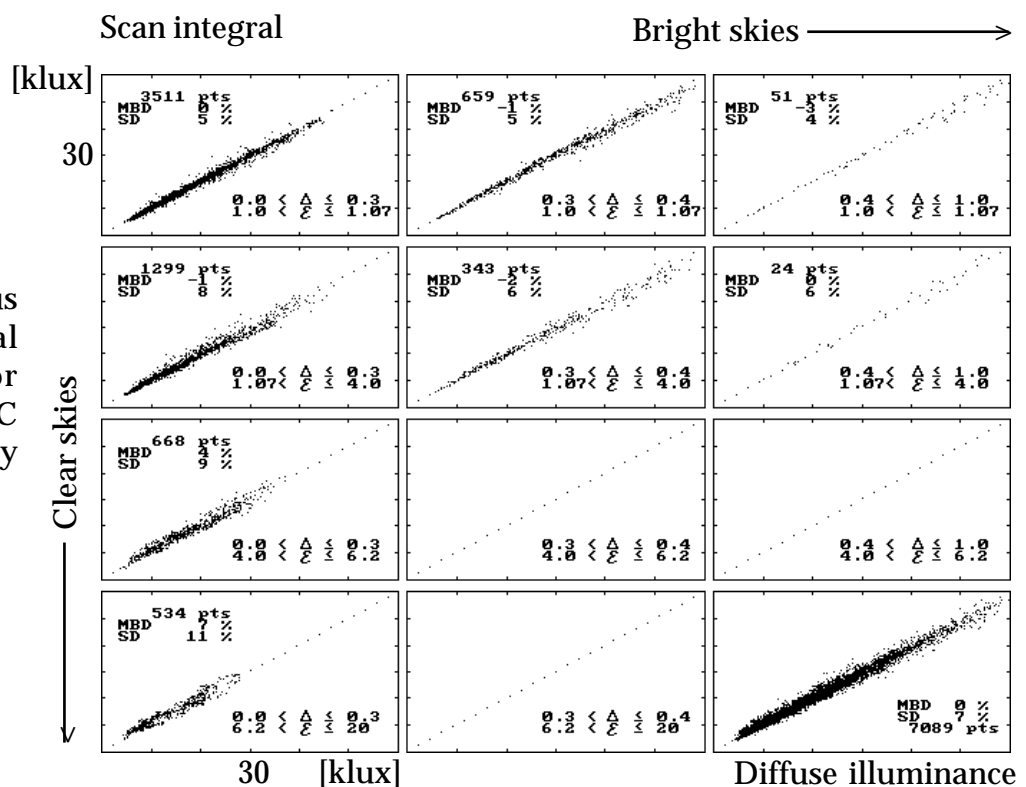


Figure 1

Scan integral versus diffuse horizontal illuminance for Geneva, PRC Krochmann sky scanner

Figure 2

Scan integral versus diffuse horizontal illuminance for Geneva, EKO Instruments sky scanner. For these measurements, we had to apply a 17% correction on the manufacturer calibration's factor

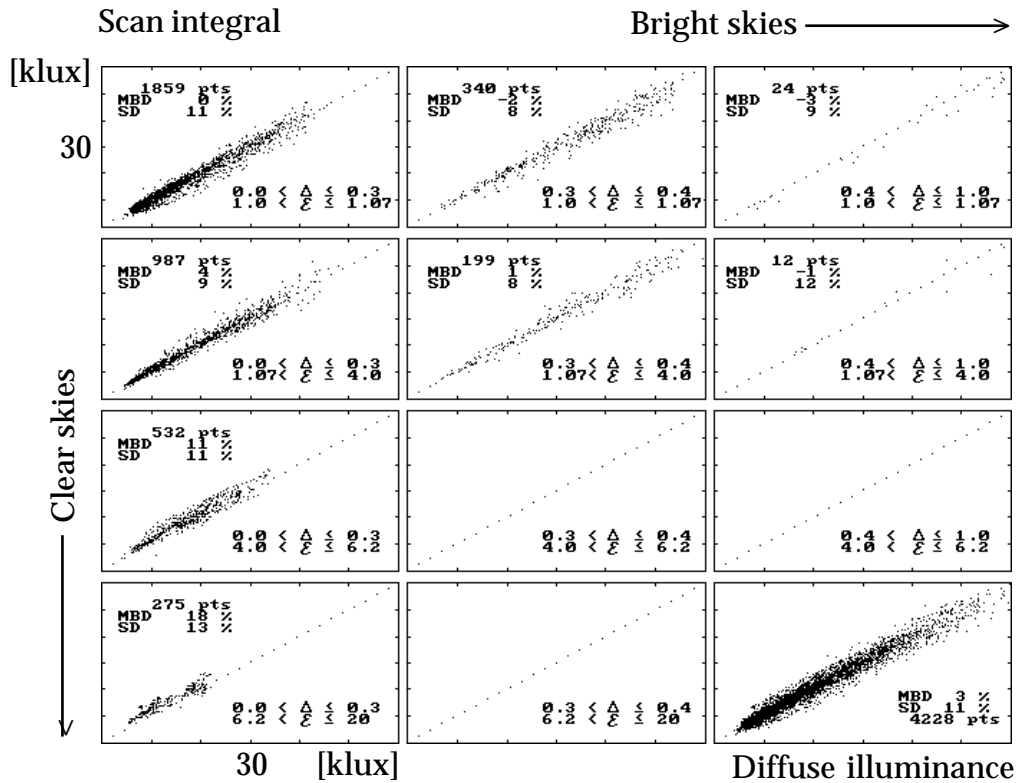
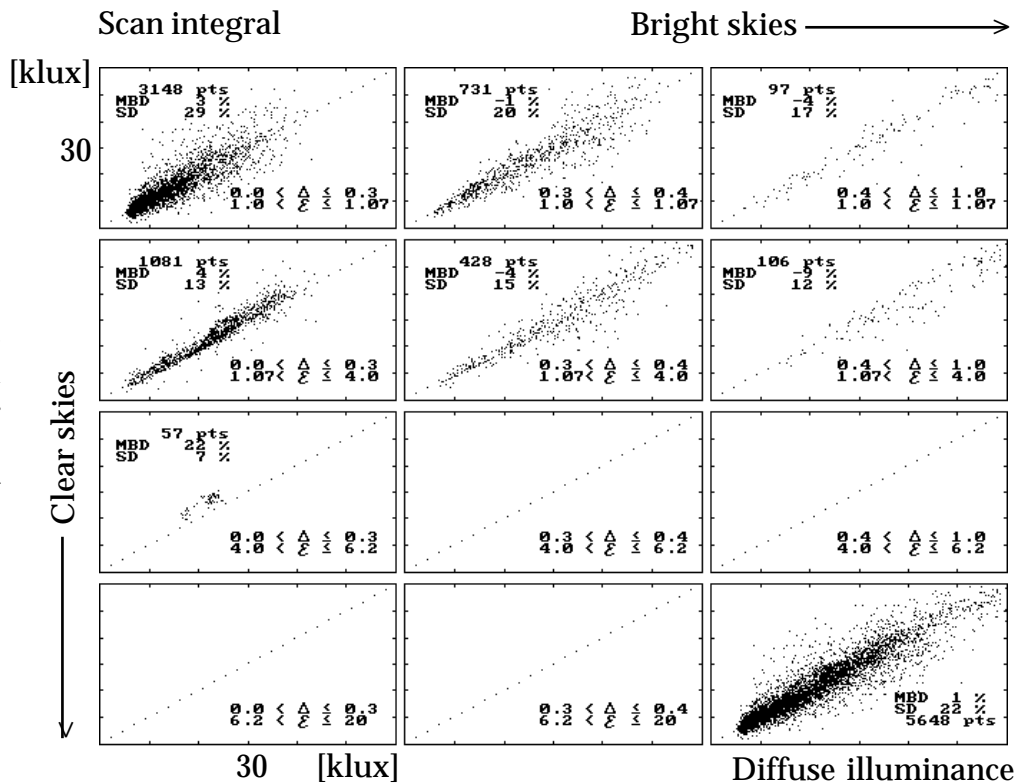


Figure 3

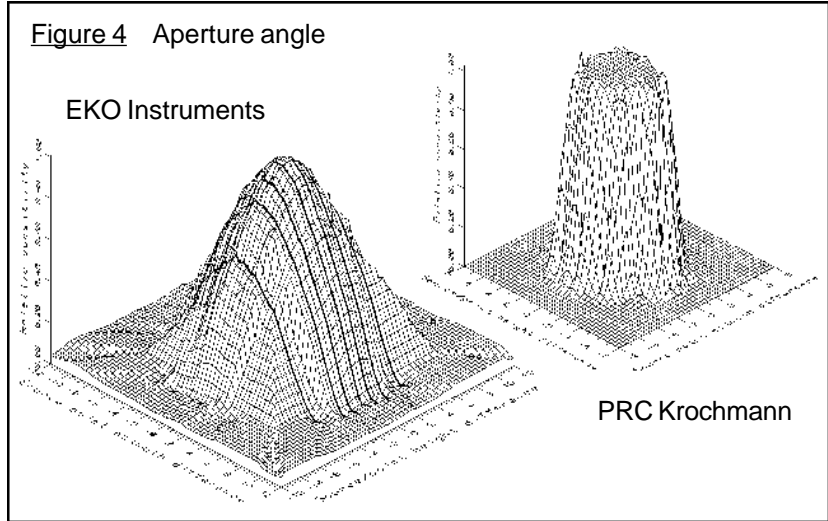
Scan integral versus diffuse horizontal illuminance for Garston, PRC Krochmann sky scanner



direction and the sun) have to be skipped in the integral calculation. To avoid systematic calibration bias due to the proximity of the sun, we splitted our data in sky clearness and sky brightness bins (Δ and ϵ , Perez 1987). The graph on the top and the left of Figure 1 to 3 will be the reference for our calibration quality control, these conditions are representative of dark overcast skies, with no high luminance increase in the sun direction. Figures 1, 2 and 3 give respectively the results of this comparison for PRC Krochmann Geneva's data, EKO Instruments Geneva's data and PRC Krochmann Garston's data.

We made the same quality control for all the data. The following can be pointed out from these figures:

- ✓ in the Geneva PRC data set, the influence of the sun is not negligible and there is a systematic bias for high epsilon (7%), the bias increases with epsilon,
- ✓ in the Geneva EKO figure, we trace the higher dispersion of the scatter plots to the very bad aperture angle of the sensor optic (see Ineichen, 1993) and to the long duration of the scan (2.5 minutes versus 35 seconds for the PRC). The systematic higher bias for high epsilon is also due to the $>11^\circ$ aperture angle and the bad slope angle (Figure 4),



- ✓ concerning the Garston data, the very high dispersion can be due to the version of PRC scanner. In fact, we had the same kind of problem with the Geneva PRC scanner in 1991. We made some significative tests on this data, and represented them on Figures 5 & 6.

The PRC scanner does 6 zenith luminance measurements during a single scan. It is then possible to compare these six values and, during a clear day, find out the stability and the response of the PRC electronic. Figure 5 represents the relative variation of this zenith luminance for a very clear day in Garston: May 20, 1992. One can point out on this figure that the system sensor+electronic varies systematically up to 30% during the 35' of a scan. The relative signal variation has a very repetitive pattern. We then represented on the top of Figure 6 the mean relative variation for the measurement 145 to 150, for the 1992 data, different delta bins and a specific epsilon bin (intermediate conditions, 1.9 -> 4). The points represent the mean value, surrounded by \pm one standard deviation. On the bottom of the same figure, we represented the relative value of the measurement done just before and just after each of the zenith luminance measurements, also surrounded by \pm a standard deviation. One can

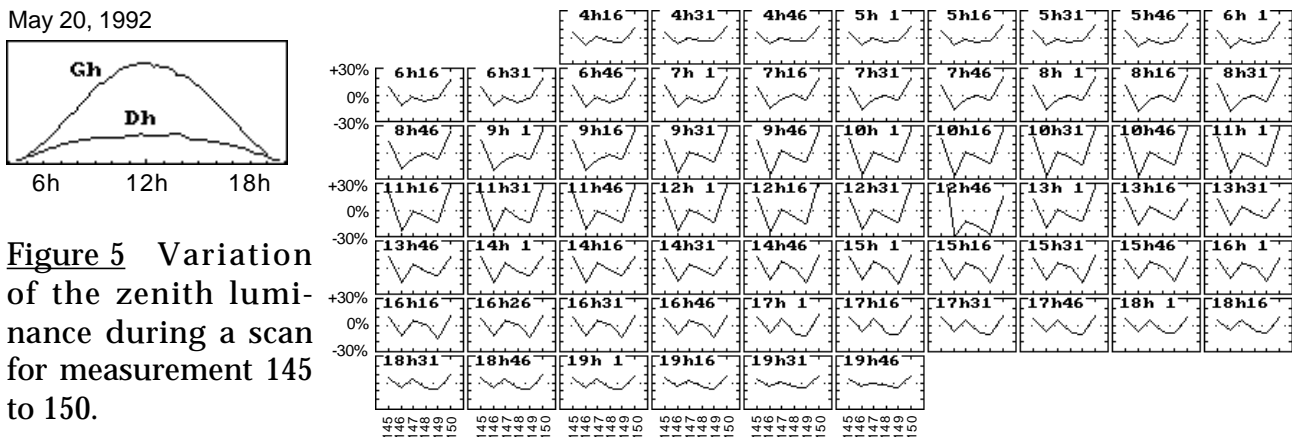


Figure 5 Variation of the zenith luminance during a scan for measurement 145 to 150.

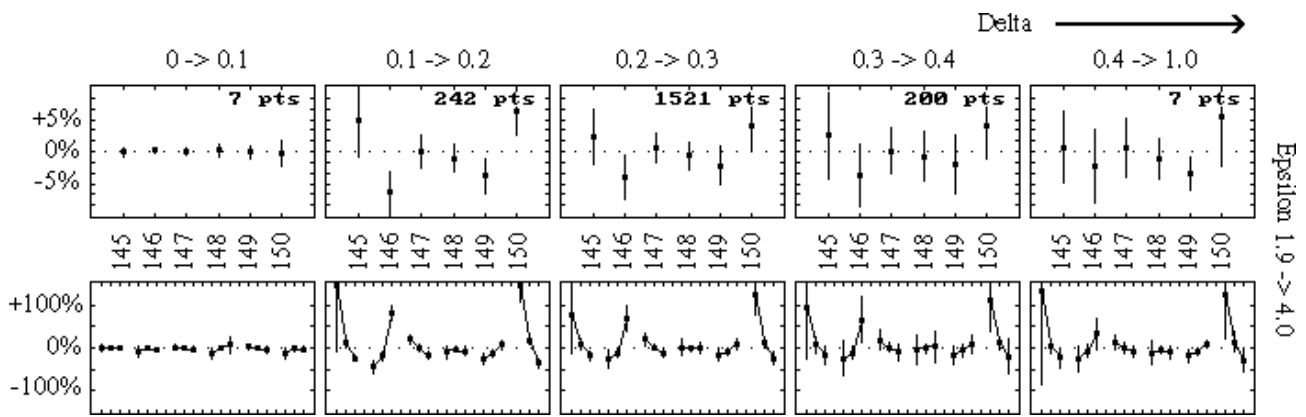


Figure 6 top: relative variation of the zenith luminance measurements during the scan, normalised by their average.
 bottom: same representation, but with the measurement done just before the zenith luminance and just after.

easily conclude that the electronic is too low in regard to the scan velocity and that each value of the scan keeps in memory a part of the preceding measurement.

This can explain the high dispersion in Figure 3. We had this problem with the Geneva's PRC scanner and it was solved by the replacement of the amplifying electronic. The manufacturer also developed a new optic for the PRC scanner after a characterisation we made in 1991 (Ineichen 1991).

In conclusion, a good knowledge of the instrument used for the measurements is very important and crosschecks between interdependent data is essential.

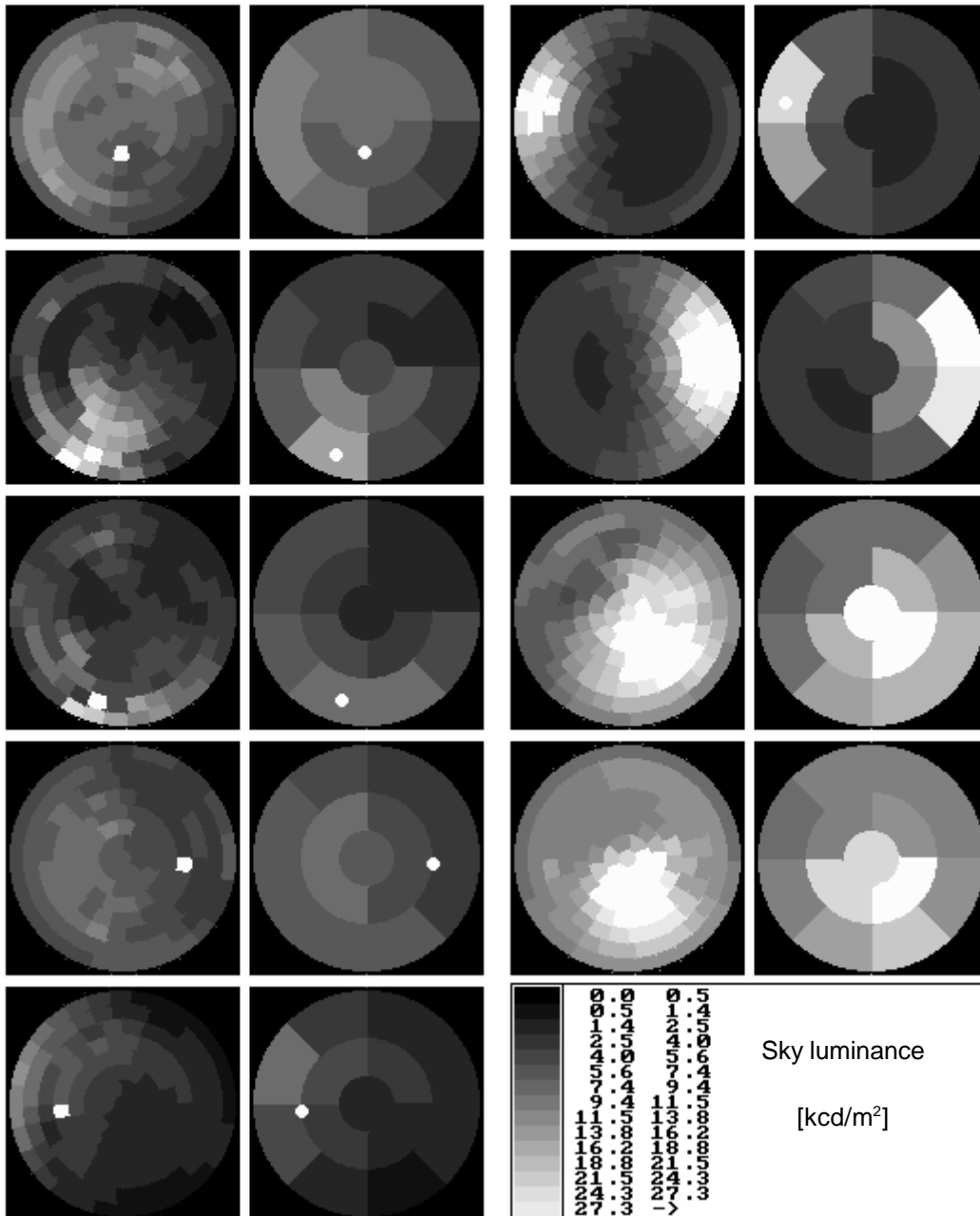
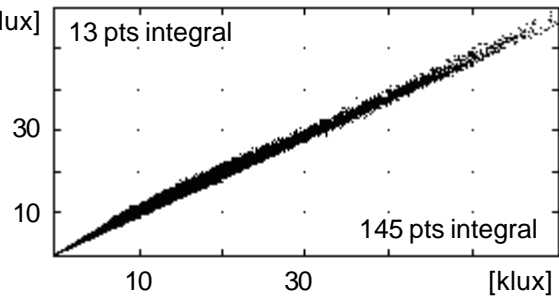
Conversion of the data

In the field of indoor daylight simulation, the space resolution of the sky luminance data can be much lower than the 145 CIE solid angles. In fact, three different altitude zones are enough to obtain a sufficient precision: a horizon band, a zenith zone, and an intermediate band. The horizon band is divided in 8 zones, the intermediate band in 4 zones. Each zone has the same solid angle. Furthermore, the CIE zones have the first measurement in the sun's meridian, whereas the 13 zones have a fixed orientation. We have then to integrate the 145 CIE values and re-orient them to adjust the measurement to the present project. Moreover, the space resolution of the meteosat data is too low to deduce a 145 zones model.

To do this conversion, we had to find out the limit angle for zeta for which the integral of the scans is only slightly influenced by the circumsolar "noise", whatever the sky conditions are. Figure 7 illustrates this conversion for some particular conditions. The white circle represents the direction of the sun. The graph represents the new 13 zones' integral versus the 145 points' integral. We obtain a diagonal scatter plot with a very low dispersion and we can then consider that the conversion did not induce a significant degradation of the data. One can observe that it is not anymore necessary to take a particular care to the "patch" that includes the sun.

We then made again the plot from Figures 1 in order to confirm the above results. The results are given in Figure 8, where a slight degradation in the calibration constant is visible on the top-left graph.

Figure 7 Conversion from 145 points to 13 zones data. The graph on the top represent the 13 zones integral versus the 145 zones integral for Geneva's data, 1994.



The indirect way from pixels to luminance

The indirect way to go from pixels to luminance distribution is to use the modelled illuminances and/or irradiances. As the existing models were tested on the 145 zones' measurement, it is interesting to re-evaluate these models with the new data set in order to find out the best adapted model to the meteosat problem.

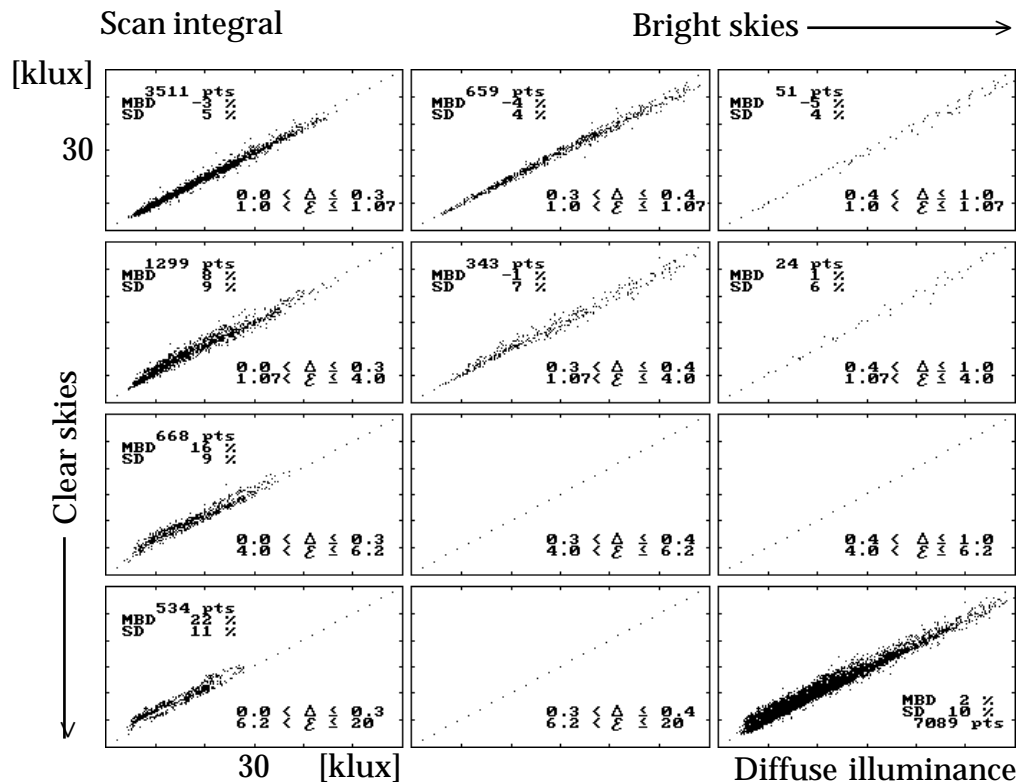


Figure 8

Scan integral versus diffuse horizontal illuminance for Geneva's converted data.

Brief description of the models

Most of the models described hereafter are summarised and the algorithm given in a publication from (Perez 1990):

Isotropic hypothesis

In this case, the same luminance is attributed to each sky vault zone, and the integral is then normalised by the horizontal diffuse illuminance.

Brunger model (Brunger 1980)

The model is a three components continuous model and was originally developed for modelling the sky radiance; it is a superposition of three distinct terms, isotropic, circum-solar and horizontal brightening factor. The weighting parameters are D_h/G_h and the clearness index K_t .

Matsuzawa-Iwata model (Matsuura 1990)

This model is a combination of the three CIE standard skies: clear, intermediate and overcast. The governing parameter is an illuminance "cloud ratio" defined as D_{vh}/G_{vh} .

ASRC-CIE (Perez 1992)

Perez et al. modified Matsuzawa-Iwata's model to take into account the high turbid intermediate skies. The interpolating parameters are Perez' epsilon and delta (clearness and brightness) coefficients.

Perez Model (Perez 1993)

Five coefficients describe the quality and the quantity of the luminance of the sky dome; each of the coefficients has a specific physical effect and depends on epsilon and delta: (a) darkening or brightening of the horizon region, (b) luminance gradient near the horizon, (c) relative intensity of the circum-solar region, (d) width of the circum-solar region and (e), the relative back scattered light.

Perraudeau model (Perraudeau 1990)

The formulation of the model is a product of three functions, depending respectively on the angular distance to the sun (zeta), the height of the considered point and the sun height. The five discrete sky conditions are parameterised with a nebulosity index I_n , which is a normalised cloud ratio.

Harrison model (Harrison 1991)

The model needs an opaque cloud cover (Combes 1985) to combine two basic luminance distributions: clear and cloudy sky. We used a normalized diffuse fraction as opaque cloud cover.

Kittler model (Kittler 1986)

The model is based on the light diffusion theory, it is a complex formula that calculates the absolute or relative sky luminance pattern. The governing parameter is the atmospheric illuminance turbidity.

Gueymard model (Gueymard, 1986)

For clear sky conditions, the sky luminance normalised by the diffuse illuminance, has been empirically formulated as a function of the Angstrom turbidity coefficient. A ponderation with the opac cloud cover (Gueymard 1987) is then made to take into account of the meteorological conditions.

We compared these models on the 1994 Geneva's data bank and obtained the results given in Figure 9. The evaluation method is described in (Ineichen 1994). The highlight from these figures is that the first rank is obtained by the modified CIE model and therefore, this will be the model we will use as reference in the development of our "direct" model.

The direct way from pixels to luminance

The objective of this subtask is to try to develop a direct model from the pixels to the sky distribution luminance. We will have at our disposition satellite data for the site of Geneva for one year (1994). The data are in latitude/longitude pixels, for the visible and the infrared regions. The visible pixels are converted from reflectance to nebulosity by the use of ground albedo; the infrared pixels are converted to absolute temperatures and are representative of the altitude of the clouds' top. For the model development, we will use ground measurements from our station, and synoptic data obtained from the Swiss Institute of Meteorology, acquired at Geneva's airport, not far from our station (IEA Task XVII, 1994).

We represented these informations for a single measurement on Figure 10.

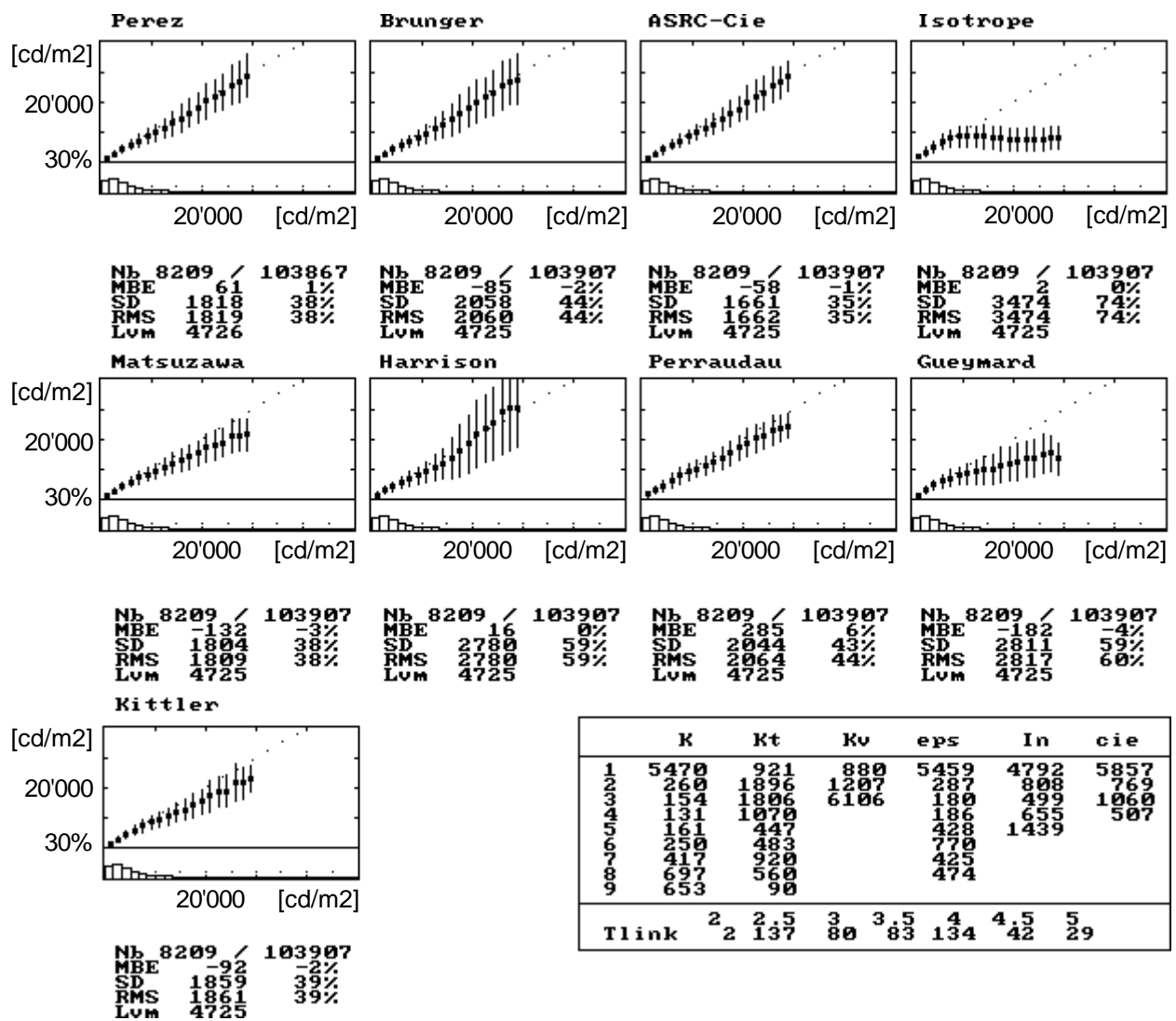
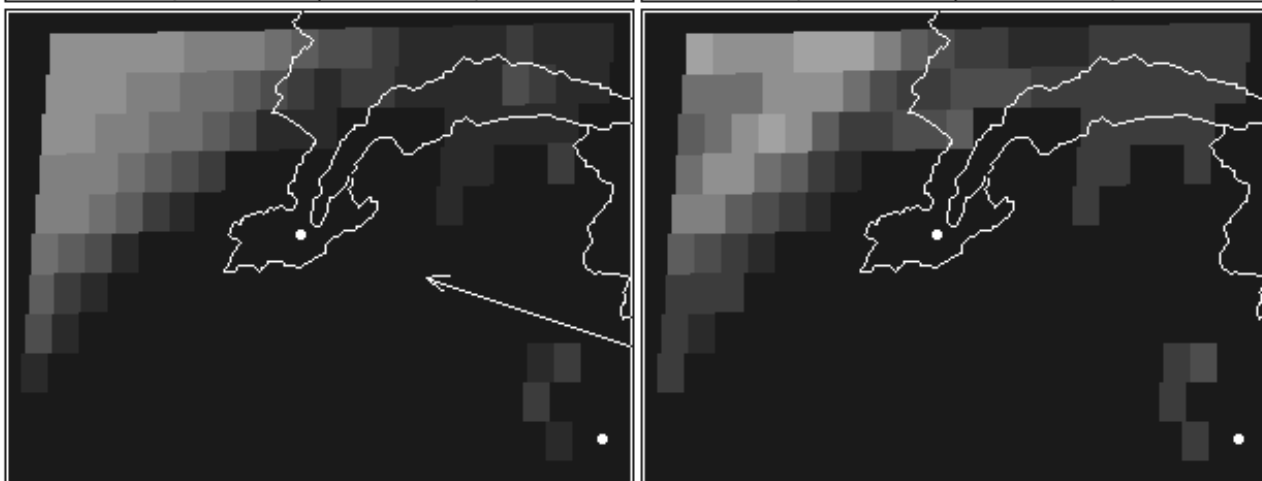
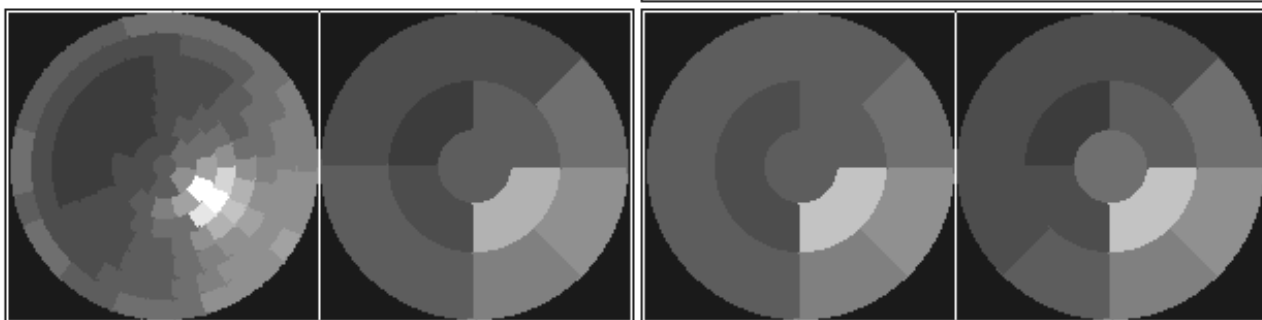
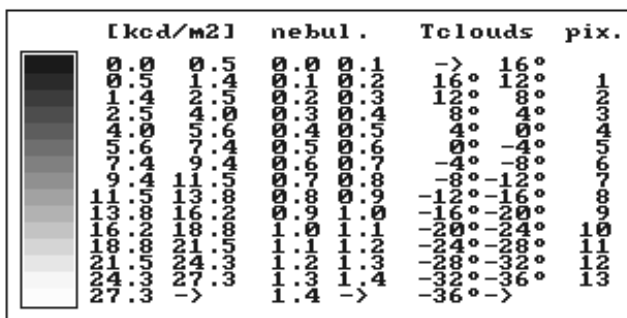


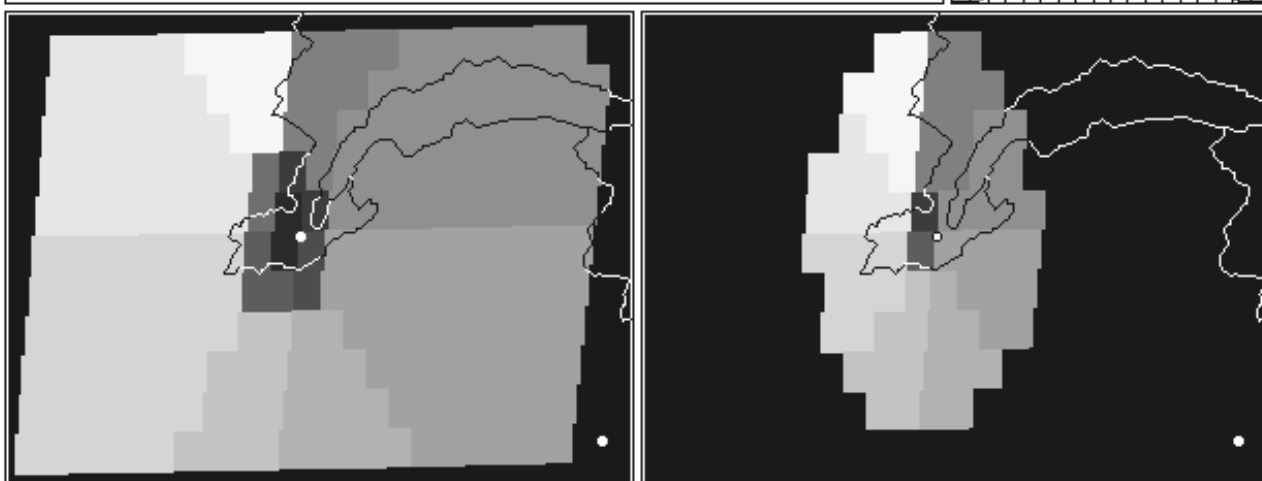
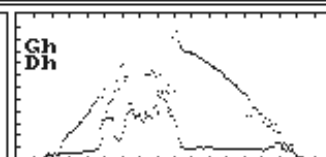
Figure 9 Evaluation of the different sky luminance distribution models on the Geneva's converted data base for the year 1994. On the bottom-right table are given the number of occurrence in each bins.

- ✓ On the top-left, we represented the 145 measurements' points and the 13 zones corresponding converted data,
- ✓ In the middle, one can find the two satellite pictures, in low resolution: on the left the nebulosity and on the right the temperature. The two white circles represent the coordinates of the ground station and the Mt-Blanc (4807m), the white arrow on the left image represents the sun rays direction. The different values corresponding to the grayscales are given on the top-right of the figure,
- ✓ The two bottom figures illustrate the pixels involved in the field of view of the sensor for two different altitudes (9000m and 3000m) and show clearly that these images will not bring enough information in the low resolution mode. The high resolution satellite images have 2.5x2.5 km pixels and are available at a hourly rate (instead of a half-hourly rate),
- ✓ the middle of the figure illustrate the global and diffuse horizontal radiation for the considered day (right graph), the ground measured and derived quantities, the synoptic data, the minimum and maximum cloud temperatures (Tc), the estimated ground

Figure 10 Sky luminance distribution as measured, converted, modelled from ground measurements, modelled from pixels, satellite picture in the visible and the IR region, ground measurements and pixels to be used in the modelisation for two clouds altitude and for the 13 zones.



8 juil 94	4 octas	Ta	20.2°	Gh	679	ma	1.30
nb.	9h 9'	Td	7.4°	Dh	243	nb	0.02
ir.	9h 9'	W	1.6cm	Bn	599	kt	0.69
lum	9h 5'	Tg	-12°	δ	0.23	k'	0.72
scan	9h 5'	Tc<	-13°	Σ	2.78	In	0.76
		Tc>	13°				



temperature (T_g), the estimate altitude of the clouds and the average nebulosity derived from the 4 pixels above the station,

- ✓ the third graph on top of Figure 10 illustrate the luminance distribution obtained with the modified CIE model and based on the ground measurements (Dh, Bn and Lvz).

With a limited low resolution Meteosat data bank (5 months), we tried to correlate the pixel information and the luminance distribution.

A first step is to evaluate the altitude of the cloud cover. The infrared information gives the absolute temperature of the clouds and/or the ground. We averaged the temperature on the cloudless pixels to obtain an estimated ground temperature, and then estimated the altitude of the clouds with a constant temperature gradient. The obtained value can be compared with the synoptic data, taking into account that the latter are on a three hour basis and give the bottom of the cloud cover.

A second step is to use the nebulosity index and to relate it with the radiation parameters. We tried to use the same index than for many other models: the sky clearness and the brightness. With the restricted data bank we obtained the distribution given in Figure 11.

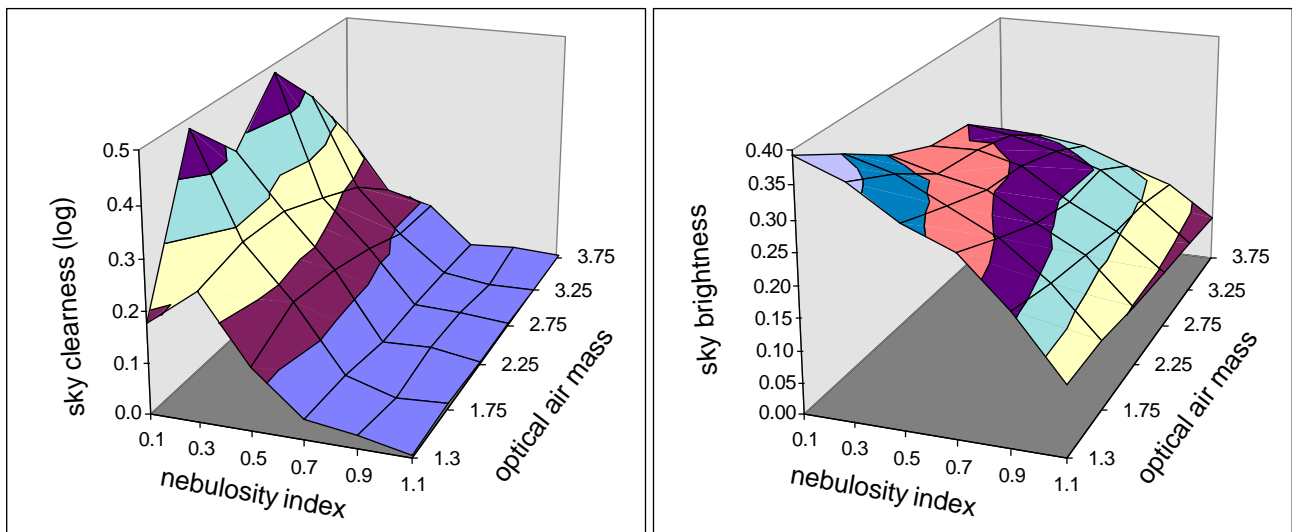


Figure 11 Behaviour of the sky clearness and brightness with the optical air mass and the nebulosity index for the limited data set.

These surfaces give tendencies and cannot be taken as correlations in the actual stage of the research. Using a "box model", we obtained the fourth representation on the top-right of Figure 10. On a 16 degrees grayscale graph, the results appears to be acceptable. At the present stage, this will certainly not be the case on a modelled/measured graph.

The development of such a model will need higher resolution meteosat pictures over at least a year and its precision and validation can only be assessed by a large scale evaluation on data from other sites.

Nomenclature

Io, Ivo	extraterrestrial irradiance and illuminance on a plane tracking the sun,
Z	solar zenith angle,
ma	optical air mass,
Gh,Dh	global and diffuse irradiances on a horizontal plane [$W \cdot m^{-2}$],
Bn	beam irradiance on a plane tracking the sun [$W \cdot m^{-2}$],
Gvh,Dvh	global and diffuse illuminances on a horizontal plane [lux],
Bvn	beam illuminance on a plane tracking the sun [lux],
Lvm, Lvm	measured luminance, average Lvm [$cd \cdot m^{-2}$],
Lvz	zenith luminance [$cd \cdot m^{-2}$],
Ta, Td, Tg, Tc	ambient, dew point, ground and cloud temperature,
Kt, Kt'	clearness index, enhanced clearness index (Perez, 1990'),
K, Kv	Dh/Gh, Dvh/Gvh,
In	Perraudé index (Perraudé, 1990),
nb	nebulosity index,
zeta	angular distance between the considered point and the sun,
delta, δ , Δ	Perez' brightness index,
epsilon, ϵ	Perez' clearness index.

References

- A.P. Brunger, F.C. Hooper, (1980)
A Model for the Angular Distribution of Sky Radiance.
J. of Solar Energy Engineering, Transaction of the ASME, Vol. 102, pp196-202, 1980.
- CIE 108-1994
Guide to Recommended Practice of Daylight Measurement.
TC-3.07, ISBN 3 900 734 50 X, Vienna, Austria
- C.A. Combes, A.W. Harrison (1985)
Radiometric Estimation of Cloud Cover.
J. of Atm. and Oc. Technology, Volume 2, N° 4, pp. 482-490, 1985.
- IEA Task XVII (1994)
Broad Band Visible Radiation Data Acquisition and Analysis.
Subtask E, Volume 2, Satellite report 1, World Network of Daylight Measuring Stations.
- C. Gueymard (1986)
Une paramétrisation de la luminance énergétique du ciel clair en fonction de la turbidité
Atm.Océan, 24 (1), pp 1-15, (1986)
- C. Gueymard (1987)
An Anisotropic Solar Irradiance Model for Tilted Surfaces and its Compariosn with Selected Engineering Algorithms.
Solar Energy, Vol. 38,N°5 , pp 367-386 (1987)
- A.W. Harrison (1991)
Directional Sky Luminance versus Cloud Cover and Solar Position.
Solar Energy, Vol. 46, N° 1, pp. 13-19, 1991

J.E. Hay, 1978

Calculation of the Solar Radiation incident on an inclined Surface.

Proc. 1st Canadian Solar Radiation Data Workshop, Toronto, 1978

P. Ineichen, B. Molineaux, (1993)

Characterisation and Comparison of two Sky Scanners: PRC Krochmann & EKO Instruments.

IEA Task XVII expert meeting, Geneva, Switzerland, August 1993.

P. Ineichen, B. Molineaux, R. Perez (1994)

Sky Luminance Data Validation: Comparison of Seven Models on Four Data Banks.

Solar Energy, Vol. 52, N°4, pp 337-346 (1994)

R. Perez, R. Seals, P. Ineichen, R. Stewart, D. Menicucci. (1987)

A new Simplified Version of the Perez Diffuse Irradiance Model for Tilted Surfaces

Solar Energy, Vol. 39, pp.221-231, 1987

R. Perez, P. Ineichen, R. Seals, J. Michalsky, R. Stewart. (1990)

Modelling Daylight Availability and Irradiance Components from Direct and Global Irradiance.

Solar Energy, Vol. 44, N° 5, pp 271-289. (1990)

R. Perez, P. Ineichen, R. Seals, A. Zelenka (1990)

Making full use of the Clearness Index for Parametrizing hourly insolation conditions.

Solar Energy, Vol. 45, N° 2, pp111-114. 1990.

R. Perez, J. Michalsky, R. Seals. (1992)

Modelling Sky Luminance Angular Distribution for Real Sky Conditions. Experimental Evaluation of Existing Algorithms.

Journal of the Illumination Engineering Soc. J. Vol. 21,2 pp 84-92 (1992).

R. Perez, R. Seals, J. Michalsky (1993)

An All-weather Model for Sky Luminance Distribution.

Solar Energy, 1993

M. Perraudau (1990)

Daylight Availability from Energetic Data.

CIE Daylighting Conference, Moscow, October 1990

R. Kittler (1986)

Luminance Model of Homogeneous Skies for Design and Energy Performance Predictions.

2nd Int. Daylighting Conference, Long Beach, CA, 1986.

K. Matsuura, T. Iwata (1990)

A Model of Daylight Source for the Daylight Illuminance Calculations on all Weather Conditions.

CIE Daylighting Conference, Moscow, October 1990